RESEARCH ARTICLE

Atomistic simulations of plasma catalytic processes

Erik C. Neyts (✉)

Research Group PLASMANT, Department of Chemistry, University of Antwerp, Universiteitsplein 1, 2610 Wilrijk-Antwerp, Belgium

Abstract There is currently a growing interest in the realisation and optimization of hybrid plasma/catalyst systems for a multitude of applications, ranging from nanotechnology to environmental chemistry. In spite of this interest, there is, however, a lack in fundamental understanding of the underlying processes in such systems. While a lot of experimental research is already being carried out to gain this understanding, only recently the first simulations have appeared in the literature. In this contribution, an overview is presented on atomic scale simulations of plasma catalytic processes as carried out in our group. In particular, this contribution focusses on plasma-assisted catalyzed carbon nanostructure growth, and plasma catalysis for greenhouse gas conversion. Attention is paid to what can routinely be done, and where challenges persist.

Keywords atomic scale simulation, plasma-catalyst

1 Introduction

The concept of combining a plasma with a catalyst to enhance the intended process relative to either the purely thermo-catalytic process or the non-catalyzed plasma process is relatively new. The first reports on combining a plasma with a catalyst were put forward by Devins et al. in 1954 for hydrazine formation [1] and by Henis in a 1976 U.S. patent for NO_x removal [2], i.e., only some 40–60 years ago, while plasma and catalysis have individually been around much longer indeed, about 300 years and 200 years, respectively [3]. Consequently, while both the plasma and the catalysis fields are quite mature, plasma catalysis as a field has only recently escaped its scientific infancy.

As is typically the case with new research fields and research topics, many of the earlier reports are mostly reporting on the phenomenon, based on the technically easier observations. Only in a later stage, researchers aim to dig deeper into the topic, address the more fundamental questions and issues, and start to employ less obvious techniques. This is typically true both for experiments and computations. It thus comes as no surprise, that it took until the turn of the millenium before the first simulations on the topic appeared [4,5].

Addressing specific plasma-surface interactions in simulations is however a far-from-trivial task, to a good extent due to the complexity of the system, and in particular due to the occurrence of inherently multi-scale multi-level phenomena. Indeed, the plasma itself is already a quite complex system, consisting of molecules, atoms, radicals, electrons, positive and negative ions, photons, and electromagnetic fields. When the plasma comes into contact with a surface, all of these factors complicate the system with respect to the standard gas-surface interaction. The system is rendered even more complex when the surface is a catalytic material [3,6].

In the context of modeling plasma-catalyst interactions, this results in a two-fold difficulty: how to address the discrepancy in accessible time and length scales with respect to the experimental setup, and how can the different plasma-specific factors be addressed? Consequently, different modelling approaches have been proposed, operating in the nanoscale to macroscale range. In particular in atomic scale simulations, both issues are quite pertinent [7].

In the past 8 years, we have worked towards addressing these issues. This contribution thus provides an overview of the work carried out so far, in particular in the field of the growth and modification of carbon nanostructures and plasma catalysis. Also the remaining issues are touched upon.

2 Scope of atomic scale simulations

Before describing the results obtained so far, it is informative to briefly review the scope and bottlenecks

of atomic scale simulations, in particular in relation to dealing with plasma-catalyst interactions.

Atomic scale simulations can be divided in essentially two types: quantum-based methods (including both wave function-based methods and density functional based methods), and classical models. Classical models can be further subdivided in reactive models, in which chemicals bonds can break and form in the course of the simulation, and non-reactive models. As the goal of any plasma/catalyst system is invariably to convert reactants into products, it is a requirement that the simulation allows to follow how chemical bonds break and form.

Therefore, the atomic scale study of plasma-catalyst interactions either requires a quantum-based method, or a reactive classical model. Many quantum-type calculations in heterogeneous catalysis are of the density functional theory (DFT) type. Indeed, while current state-of-the-art wave function-based methods are more accurate, DFT allows to work with much larger systems, containing several hundreds of atoms. If many more atoms are needed to represent the system, however, one needs to resort to classical models.

In classical models, a force field (or interatomic potential) is assumed to accurately represent all possible interactions between the atoms and molecules in the system. This, in turn, usually leads to rather complex and highly parametrized functional forms representing the interatomic interactions. The advantage is that classical simulations are much faster compared to DFT and can therefore handle much larger system, but the disadvantage is that they are significantly less accurate.

When a method (quantum-based or classical) is chosen, there is another fundamental issue to be addressed: the accessible time scale. Any chemical process that has an appreciable reaction barrier relative to the operating temperature will require a prohibitively long calculation time to be observed in the simulation. Indeed, typical DFT-based molecular dynamics (MD) simulations are limited to a few tens of picoseconds, which is much too short to observe essentially any thermally activated process. Therefore, most DFT calculations are static, e.g., calculating the barrier for a given process, without actually following the atoms through space and time. Classical MD simulations allow to follow processes on longer time scales, typically in the order of tens or hundreds of nanoseconds, but this is still well below the time scale of many processes.

Simply raising the temperature, in order to speed up the processes to be observed, is not a viable option, as this alters the relative rates of processes. Through the years, several methods have been devised. Well-known methods include parallel replica [8,9], hyperdynamics [10,11] and temperature-accelerated dynamics [12,13]. Recently, we developed in our group a highly efficient and generic variant of hyperdynamics, called collective variable-driven hyperdynamics (CVHD) [14]. This method allows to extend the accessible time scale by up to 9 orders of magnitude, into the seconds time scale, even for chemically complex systems [15,16].

After having chosen a method to tackle the problem, and addressed the issue of the time scale, the question arises: how to address the many plasma-specific factors in an atomistic simulation? Some of these factors are rather easy to incorporate, such as the interaction of radicals (instead of molecules) with the catalyst; for others there is no suitable technique or method reported yet, such as the interaction of vibrationally excited species with the surface; and for still others, techniques exist, but are very time-consuming, such as the interaction of electronically excited species, requiring time-dependent DFT (TD-DFT). The interested reader is referred to a recent review for a more elaborate discussion of this issue [17].

In the following sections, the focus lies on the application of both classical and quantum atomic scale simulations to model plasma catalytic processes, encompassing both the growth of nanocarbon structures as well as plasma catalytic processes.

3   Atomic scale simulations of plasma catalytic processes

3.1   Plasma catalytic carbon nanotube growth

There is a rich literature on the atomic scale simulation of the catalyzed growth of carbon nanotubes (CNT) and related materials such as graphene and fullerenes [18–24]. As the most common growth technique for CNTs is (thermal) chemical vapor deposition, most simulation studies also refer to this technique [25,26]. Thus, there are so far not many simulation studies specifically addressing plasma enhanced chemical vapor deposition (PECVD) of CNTs. Nevertheless, it is well known that plasma-based growth may offer some advantages over pure thermal growth, including a lower growth temperature, aligned growth and possible partial control over the resulting chirality. A number of excellent reviews exist on plasma catalytic growth of CNTs [27,28].

Typical thermal catalytic growth simulations essentially consist of throwing a large number of carbon atoms at the nanocatalyst. This is the usual recipe in molecular dynamics simulations [29]. The time in between two impacts is typically of the order of a few ps, which is obviously much too fast compared to the experiment. Alternatively, researchers have also performed simulations based on grand canonical Monte Carlo simulations, where not the impingment flux of the carbon is fixed, but rather the carbon chemical potential [30]. This constitutes the other extreme, and corresponds to the thermodynamic equilibrium being established in every addition step.

Whichever approach is taken, in order to simulate a plasma-based growth process, an electric field, ion

bombardment and radicals as growth species should be added to the simulation setup. Other plasma factors, such as photons, are not very likely to play an important role in the growth process. Charging, however, may be important as well.

In a first approximation, the electric field can be added as a simple one-body force, acting on all partially charged atoms. Thus, this requires the use of a force field including (variable) atomic charges. This approach was used in [31] to evaluate the effect of adding an electric field on the growth process. Importantly, it should be noted that the charge density is not modified self-consistently in response to the electric field; the electric field only displaces charge-carrying atoms. This is likely to underestimate the effect of the electric field, and therefore, quite large values for the electric field must be applied in order to observe a noticable effect.

In [31], a combination of molecular dynamics with so-called force bias Monte Carlo (MD/fbMC) [32–36] was used to (partially) include long time scale relaxation effects in the simulation. It was indeed demonstrated earlier that this is required for reducing the number of defects in the growing nanotube [20,37]. Electric field values in the range 0.1–1000 kV/cm were used, perpendicular to the surface to which the Ni nanocatalyst was attached. In the lower E-field range, between 0.1 kV/cm and 100 kV/cm, there is no noticable effect, and the CNT cap nucleates at a random position on the surface of the cluster. Increasing the E-field value to values in the range 300 to 800 kV/cm, the CNT cap preferentially nucleates near the top of the catalyst particle. Increasing the E-field even further, to values beyond 800 kV/cm, no cap nucleation is observed. This is shown in Fig. 1(a).

These observations can be explained by considering the charge separation in the Ni/C system, as shown in Fig. 1(b). As the electronegativity of carbon is significantly higher than that of nickel, the C-Ni bonds are polarized, and the carbon atoms acquire a small negative charge, whereas the Ni-atoms acquire a small positive charge. The E-field then acts on these negatively charged carbon atoms: If the random, thermal diffusion of the carbon atoms dominates the driving force of the E-field (i.e., at low E-field values and/or at sufficiently high temperature), then the carbon atoms end up nucleating a network randomly. If, however, the migration of C-atom due to the E-field near the tip of the catalyst dominates the random thermal diffusion (i.e., at higher E-field values and/or at lower temperatures), then the carbon atoms will preferentially form the C-network at the tip. This may, eventually, lead to the formation of free-standing single walled CNTs [38,39],
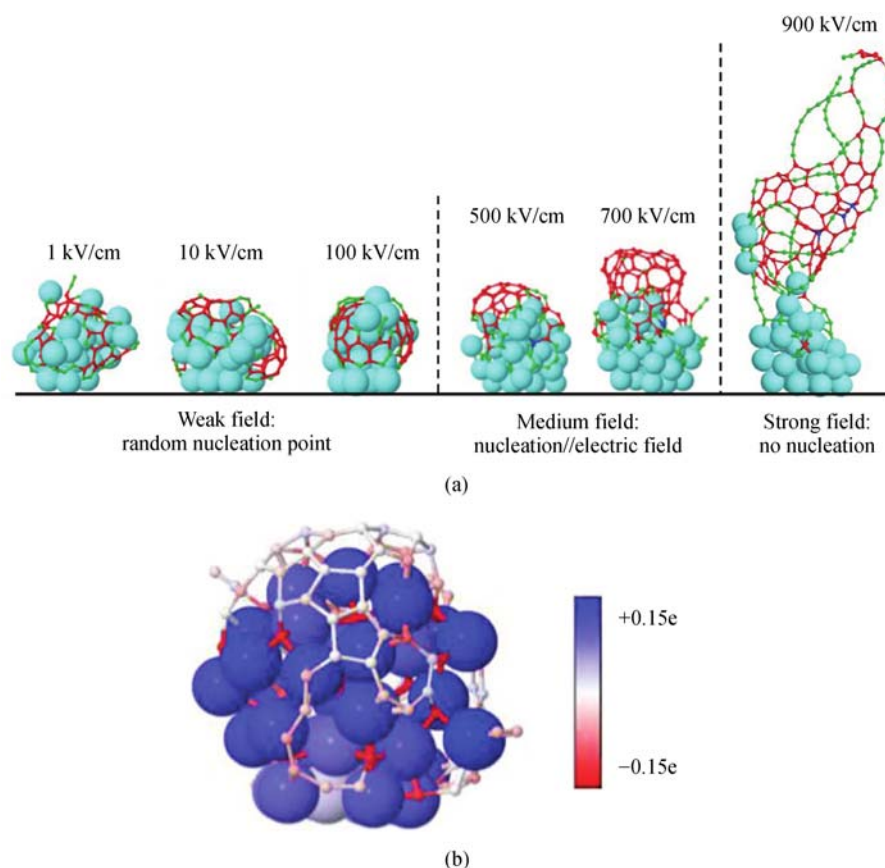

Fig. 1 Effect of adding an electric field to the Ni-catalyzed CNT growth. (a) Vertical nucleation is observed in the E-field range 300–800 kV/cm; (b) charge separation in the Ni/C nanocluster. Reproduced with permission from ACS [31]

which may be useful for, e.g., the formation of sensors.

In a plasma, the electric field also accelerates the ions to the surfaces and to the growing CNT structure. This ion bombardment may either lead to beneficial effects (e.g., elimination of amorphous carbon) or detrimental effects (e.g., sputtering of the growing CNT), depending on the exact conditions. A recent review on this topic can be found in reference [40].

In the case of the plasma catalytic growth process, it is most interesting to consider the ion-assisted growth of CNTs, i.e., the beneficial effects. During the nucleation stage of a CNT, amorphous fragments will inevitably form at the catalyst surface, as the carbon supply is intrinsically stochastic. The energy supplied by ion bombardment may, however, convert these amorphous fragments in the (desired) hexagons and thus a crystalline configuration.

In a series of simulations [41], we demonstrated how inert low-energy Ar ions, with an energy below 10 eV, do not affect the structure of the growing CNT network much. Increasing the energy to the range 10–25 eV, however, is seen to induce a healing of the CNT network. Thus, in this energy range, short polyyne chains, trimers, dimers and single C atoms are seen to become incorporated in the network. Even more importantly, defect structures (such as pentagons and heptagons) are seen to restructure into hexagons under the influence of the ion bombardment. Increasing the ion energy further, above 25 eV, leads to a sputtering of the carbon network, and thus prevents the formation of the CNT (see Fig. 2).

These simulations were complemented by matching experiments. In the experiments, an external bias voltage of a few volts to a few tens of volts was applied. Remarkably, an optimal bias energy was found at 20 eV, in terms of the graphitic G-peak in Raman spectra of nascent SWNTs. This bias voltage correlates well with the optimal simulation value of 10–25 eV.

We explain these results by observing that the energy input through ion bombardment is highly local, in contrast to the energy supply through heating. In the case of ion bombardment, only the targetted atom and its immediate surroundings are directly affected. If the transferred energy is below the bond breaking threshold energy, the network is essentially left unaltered. If, however, the transferred energy exceeds this threshold, the bond will break and may re-form with, possibly, other carbon atoms in the network. This process may therefore eventually leads to a reorganisation of the network in its most stable form, i.e., as a crystalline network. This mechanism is indeed what is observed in the simulations [41,42], as shown in Fig. 2.

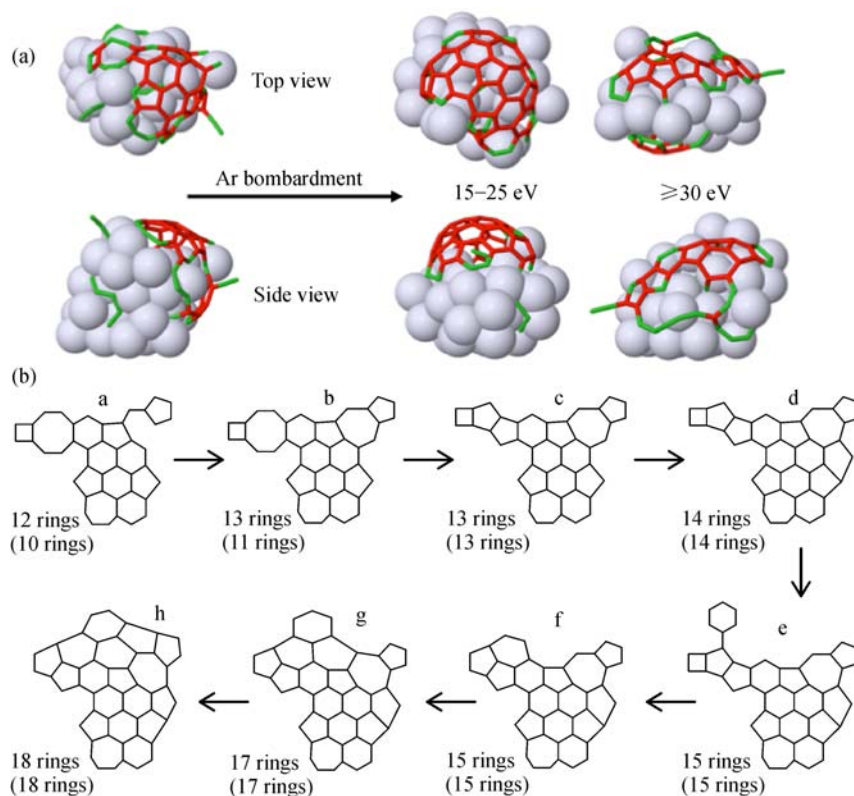Furthermore, ions may also add to the growth of the

Fig. 2 (a) Observed defect healing and enhanced cap formation by ion bombardment in the energy range 15–25 eV and destruction of the network at higher energies (> 30 eV); (b) growth of the carbon network due to the ion bombardment at 15 eV, as seen in the MD simulations. The numbers in parentheses indicate the sum of the pentagons, hexagons and heptagons; the other numbers indicate the total number of rings in the patch. Reproduced with permission from [41]

network as growth species. Thus, if carbon ions are present, they may implant in the catalyst, and thus contribute to the reservoir of C-atoms from which the CNT grows. This mechanism is of particular interest in the case of low-temperature growth, where the thermal energy is insufficient to allow for sufficient bulk diffusion of carbon atoms. This process was simulated by Shariat et al. [43,44]. In these simulations, a Fe-nanocluster was used as catalyst, and both carbon ions and thermalised carbon atoms were used as growth species. In Fig. 3, an example is shown of a CNT growing from atoms and ions (in a 4-to-1 ratio) with thermal energy and 60 eV, respectively. The blue color denotes carbon atoms that ended up in the CNT network through bulk diffusion, while the red color denotes carbon atoms in the CNT network resulting from surface diffusion.
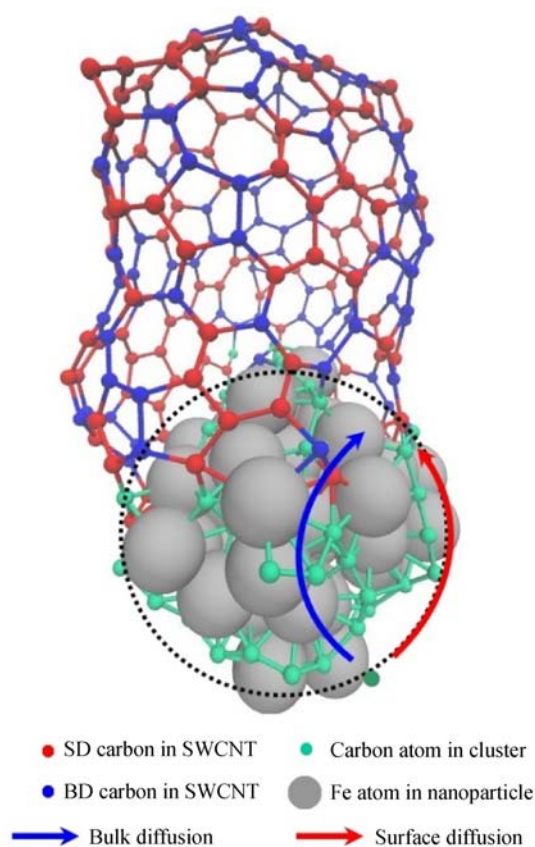

Fig. 3 Contribution of carbon atoms in the CNT network due to surface diffusion (SD) and bulk diffusion (BD), in ion-assisted growth. Reproduced with permission from [44]

These results demonstrate that insight in the plasma-based growth process of CNTs is possible through simulations. So far, however, none of these simulations addressed the interplay of the various plasma factors, and how this would affect the growth process. Therefore, an immediate challenge is to combine the application of an electric field, the presence of radicals and the presence of both precursor molecule ions and inert carrier gas ions in the simulation.

3.2   Plasma catalysis for greenhouse gas conversion

Plasma catalysis has received considerable attention in the plasma community in the last 10 years, as it is seen as a novel way to induce chemical reactions for which thermal catalysis is not favorable. Examples include the abatement of toxic waste gases (e.g., volatile organic compounds, VOCs) and the conversion of greenhouse gases into value-added chemicals (e.g., conversion of CH_4 and CO_2 to synthesis gas, a mixture of CO and H_2) [3,45,46]. Conceptually, the idea is to use a plasma to modify the source gas such that it becomes more reactive, and to use a catalyst to selectively promote the desired reaction(s) towards the end products. The source gas modification consists of decomposing it into highly reactive radicals, charged ions and electrons, and vibrationally and electro-nically excited species. While the function of the catalyst is similar to its role in thermal catalysis, it is important to realize that the plasma may effectively modify the properties of the catalyst, both morphologically and electronically, which obviously modifies the occuring surface reactions [3,6,47].

Plasma catalysis is thus quite a complex process, and modeling this process inherently requires a multiscale multilevel approach. At the atomic scale level, we so far focussed attention to the interaction of plasma-generated radicals with typical catalyst surfaces, and the effect of adding an electric field. Beyond the atomic scale level, other simulation work in our group focussed on a.o. the plasma penetration in catalyst pores [48,49] and the effect of packing [50–52].

Similar to investigating the effect of adding an electric field on the nucleation of a CNT cap (see above), we also investigated the effect of an electric field on the catalytic oxidative dehydrogenation of methanol to formaldehyde on a stoichiometric vanadia surface [53]. At a typical temperature of 650 K, however, the reaction time is far too long for the process to be observed in regular molecular dynamics simulations. We therefore applied our recently developed collective variable driven hyperdynamics (CVHD) method to extend the time scale of the simulations [14].

Over a total of 90 simulations, the average reaction time for the methanol to formaldehyde reduction is 0.69 s. There is, however, a difference in reaction time of seven orders of magnitude between the slowest observed reaction (51.4 s) and the fastest reaction (6.6 µs). A scatter plot of the reaction time, including the results for different electric field strenghts, is shown in Fig. 4.

As was the case for the CNT nucleation, also in these simulations the electric field is not modeled self-consis-tently, but rather added as an external 1-body force. It is likely that this procedure underestimates the actual effect
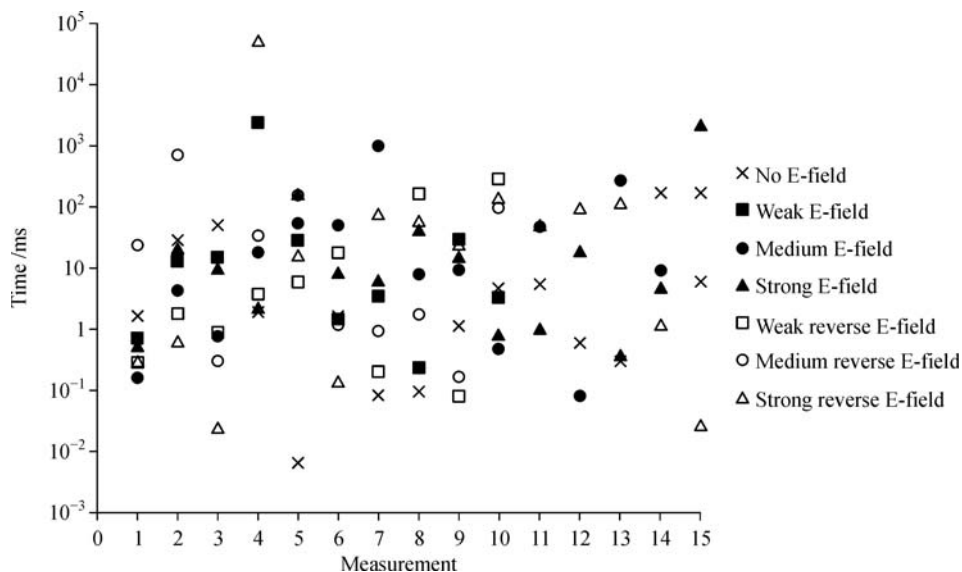
Fig. 4 Scatter plot of the time to first methanol to formaldehyde conversion in ms. Reproduced with permission from [53]

of the electric field on the process. Nevertheless, the simulations point out that when the electric field points towards the surface, the retention probability of the molecules near the surface is reduced by 6%. If the polarity of the field is reversed, the rentention time increases by almost 13%. As the retention time (at least in part) determines the surface reaction probability, it is thus clear from the simulations that the presence of an electric field — even if not affecting the reaction mechanism directly — has an important influence on the plasma-surface interaction.

The interaction of hydrocarbon plasma radicals with nickel catalysts was studied by Somers et al. [54–56]. In particular, the influence of the catalyst facetting, the surface structure, and the reaction temperature on the reaction pathways was investigated. In a first study, the reacitvity of CH, CH$_2$ and CH$_3$ radicals on Ni(111), Ni (100) and two stepped Ni(111) surfaces was studies at 400 K [54]. In agreement with the increasing number of free electrons per radical and the decreasing steric hindrance upon impact, the reacitivity sequence is found to be CH$_3$ < CH$_2$ < CH. On the stepped surfaces, additional C-H bond breaking is observed after the initial adsorption. This leads to the formation of C$_2$H$_4$, C$_2$H$_6$, and H$_2$, in particular in the case of CH$_2$ impacts. As H$_2$ is a valuable chemical, we subsequently specifically investigated H$_2$ formation in a temperature range of 400–1600 K on a Ni(111) surface [55]. However, we found that only at or above a temperature of 1400 K, significant H$_2$ formation occurs. This is not desired, since at these temperatures, carbon atoms are observed to easily diffuse into the subsurface region of the catalyst, thereby amorphisizing the crystal. Moreover, in the presence of an oxidant, the surface-adsorbed C-atoms can form CO; by diffusion into the subsurface area, however, this process is impeded and

the catalyst is deactivated. Therefore, we extended this study to investigate the temperature influence on other nickel surfaces as well [56]. These simulations demonstrate that after CH$_x$ adsorption, the subsequent C-H bond breaking depends both on the temperature and on the surface structure. In particular, the C-H bond breaking is promoted by a higher temperature, and by higher surface energy surfaces. As demonstrated earlier, too high temperatures need to be avoided. We identify a temperature range of 400–800 K as optimal. In this temperature range, the adsorbed H-atoms already react with other incoming radicals (either CH$_x$ or other H-atoms), while the carbon diffusion into the bulk of the catalyst remains low. Thus, even though little H$_2$ is directly formed at these temperatures, the fairly high reactivity between incoming radicals and adsorbed species is interesting for plasma catalytic applications.

As the plasma catalytic conversion of greenhouse gases is often studied using dielectric barrier discharges (DBD), in which vibrationally exited species are important [57], attempts were made to extend these studies to investigate the interaction of vibrationally excited CH$_4$ with the nickel surface employing classical simulations. However, these attempts were not generally successful. While certain experimental observations could indeed be reproduced, i.e., the increased reactivity of vibrationally excited CH$_4$, the magnitude of this increase relative to the reactivity in the ground state could not be reproduced. The vibrational efficiency is defined as

$$\eta_{\text{vib}} = \frac{\Delta E}{\Delta E_{\text{vib}}},$$

where ΔE is the decrease in translational energy allowing for maintaining the same adsorption probability in the vibrationally excited state as in the vibrational ground

state, and ΔE_{vib} is the vibrational excitation energy. Thus, for $\eta_{vib} > 1$, it is more beneficial to add energy to the vibrational motion of the molecule (less vibrational energy is needed than translational energy to attain a certain adsorption probability), while the opposite is true for $\eta_{vib} < 1$. Experimentally, the energy shift between the ground state and vibrationally excited state is 45 kJ/mol on the Ni(111) surface at 475 K, while the fundamental of the v_3 state has 36 kJ/mol additional energy relative to the ground state. This results in $\eta_{vib} = 1.25$, while we find in the simulations a value of $\eta_{vib} = 0.83$, corresponding to an energy shift of only about 30 kJ/mol. This is shown in Fig. 5. The origin of this discrepancy with the experimental results is probably to to a combination of several reasons, including the insufficient accuracy of the employed force field to describe vibrationally excited states, the fact that energy could not be localized in the C-H bond oriented towards the surface as is experimentally observed [58], and the influence of non-adiabatic coupling, i.e., the transfer of vibrational energy to the ground state or to a vibrational state of lower energy [59].

To avoid inaccuracies resulting from the use of classical force fields, we also perform quantum chemical studies, again to unravel the interaction mechanisms of hydrocarbon radicals with surfaces typically used in plasma catalysis. Moreover, this also allows to actual address dry reforming of methane (i.e., involving CO_2), for which no suitable classical force field is currently available.

In the simulations, the most abundant species present in the plasma were allowed to react at the Ni(111) surface, and the minimum energy path connecting the reactants and products was calculated as a function of the hydrogen surface coverage. The subsequent dissociation or desorption of the formed surface species is also investigated [60]. The effect of the surface hydrogen coverage is quite important, as the plasma dissociates hydrogen containing molecules into radicals and H-atoms. It is found that increasing the H-coverage of the Ni(111) surface facilitates the dissociation of surface-adsorbed species. For instance, an impinging O-atom reacts with a surface-adsorbed CH_3 species to form a surface-adsorbed CH_2OH species. This, in turn, is hydrogenated to methanol and desorbs though
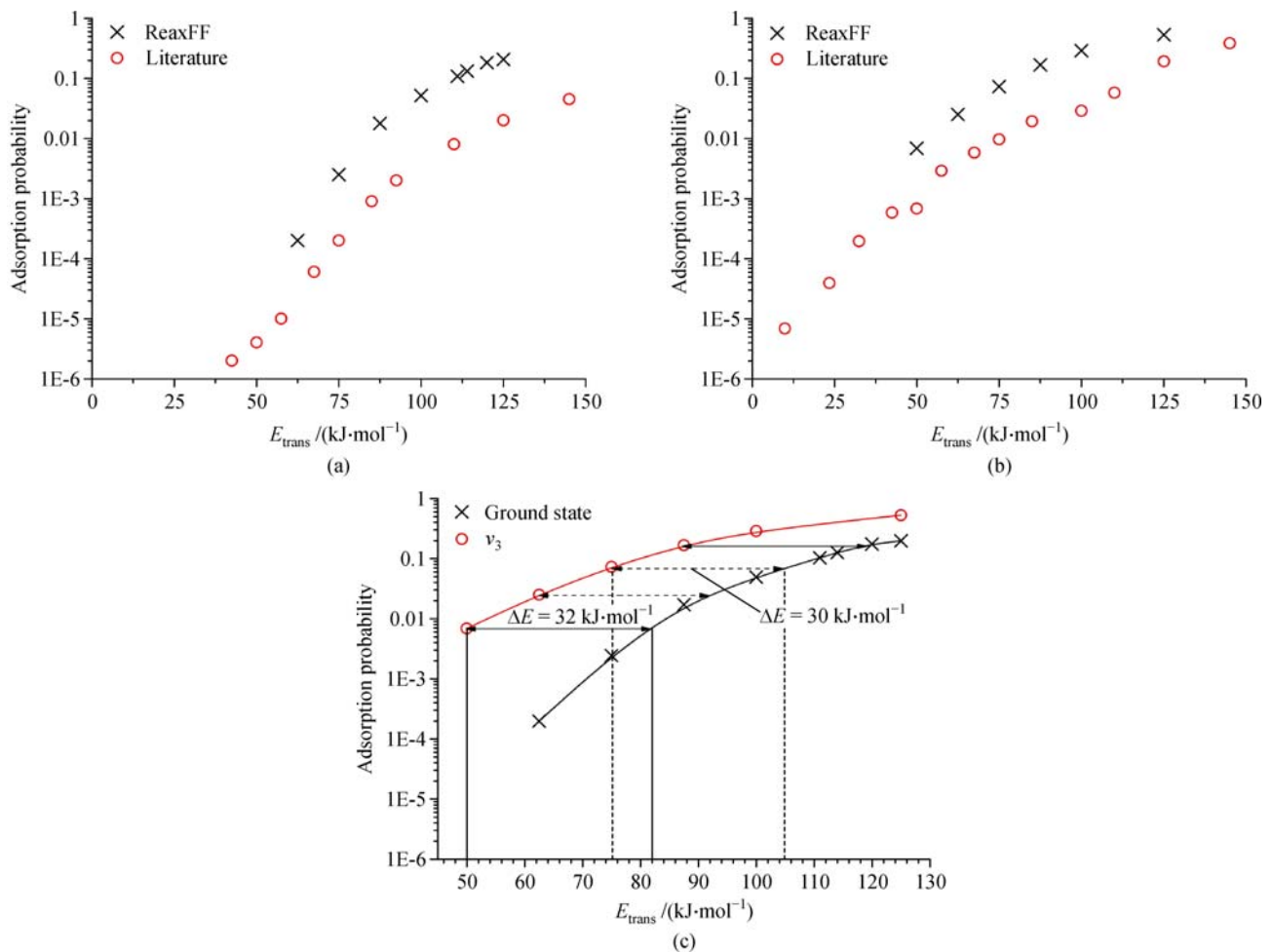

Fig. 5 Effect of vibrational excitation of CH_4 molecules on a Ni(111) surface. (a) Comparison between simulated and experimental adsorption probability for CH_4 in the ground state as a function of the kinetic energy; (b) comparison between simulated and experimental adsorption probability for CH_4 excited in the v_3 state as a function of the kinetic energy; (c) comparison of the simulated adsorption probability between CH_4 in the ground state and in the v_3 state, as function of the translational energy

the Langmuir-Hinschelwood reaction with a surface-adsorbed H-atom. The reaction barrier for the latter process is observed to decrease from 0.59 eV at a hydrogen surface coverage of 0.25 monolayers (ML) to 0.14 eV at a coverage of 0.75 ML. Similarly, the formation of CH_3OH, as well as the hydrogenation of C_1 and C_2 hydrocarbon fragments was studied as function of the hydrogen coverage. Invariably, we observe that increasing the hydrogen converage either decreases the reaction barrier to hydrogenation (in the case of open shell species) or the barrier to desorption (in the case of closed shell species). A representative example is shown in Fig. 6. Similar trends were observed for the formation of formic acid, formaldehyde and methanol, indicating that the effect of hydrogen coverage is quite general.
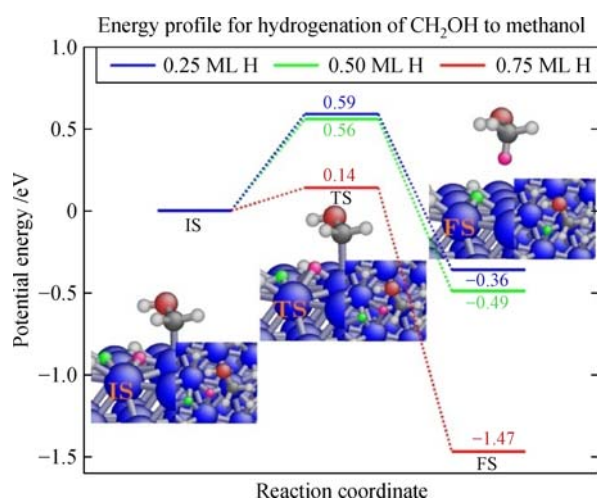

Fig. 6 Reduction in activation energy for associative desorption of methanol due to an increase of the H-coverage. Side view and top view of H-transfer (pink atom) to previously formed CH_2OH fragments are shown in the insets for a coverage of 0.75 ML of H. The associative desorption of methanol (side view) will cause the associated H diffusion at the surface (green atoms). Reproduced with permission from [60]

While nickel is an often used catalyst, also other surfaces are of significant interest in plasma catalysis. In particular TiO_2 is often considered, as its anatase polymorph is catalytically active. Thus, again employing quantum chemical calculations, we also investigated the adsorption of CH_x species on a TiO_2 (001) anatase surface, and in particular the influence of oxygen vacancies on this process [61]. First, we determined that the oxygen vacancy is preferentially located at the surface. In this case, both C and CH are less strongly adsorbed on the surface compared to adsorption on the stoichiometric surface. If the vacancy is present in the subsurface, however, all CH_x species (with $x = 0–3$) adsorb more strongly. Moreover, the presence of an oxygen vacancy is also observed to determine the adorption location. In particular, C-atoms are seen to

adsorb far away from the vacancy, CH is seen to show no preference, and CH_2 and CH_3 are seen to adsorb at the vacancy site.

The importance of oxygen vacancies in the TiO_2 surface is further demonstrated by their effect on the activation of CO_2. Indeed, we find that CO_2 can both physisorb and chemisorb on the fully oxidized surface, but not dissociate. Thus, for conversion to more useful chemicals, oxygen vacancies are required. In the presence of an oxygen vacancy, CO_2 is observed to adsorb more strongly, and lead to the dissociation of CO_2 to CO and O. The CO molecule can subsequently desorb, while the O-atom will occupy the oxygen vacancy site, thus resulting in the stoichiometric surface [62]. Calculations are currently carried out to determine the kinetics and thermodynamics of oxidation of hydrocarbon species by lattice oxygen.

Again, these results provide fundamental insight in the occurring processes, albeit for rather specific conditions. In particular, it would be of great interest to generalize these efforts, taking into account the various plasma factors contributing to the plasma catalytic process. It seems that quantum chemical calculations are most appropriate for this goal, in order to attain a sufficiently accurate description of the system.

4 Conclusions

Plasma catalysis is a complex processes, and modeling plasma catalytic processes is highly non-trivial. In this contribution, an overview is presented of the atomic scale simulations on plasma catalytic carbon nanotube growth and greenhouse gas conversion as carried out in our research group in the past 8 years. So far, most attention was paid to the reactivity of plasma generated radicals at the catalyst surface. A number of simulations were also carried out to investigate the effects of the electric field in a first approximation, as well as ion bombardment, on these processes. Future steps should involve the simulation of vibrationally excited species and the effect of charging on the occurring processes. Taking all these effects into account would result in a significant step forward in understanding plasma catalytic processes at the atomic scale. Coupling this information to higher-level models would eventually allow to design matching simulations and experiments, to gain a comprehensive understanding of plasma catalysis.

References

1. Devins J C, Burton M. Formation of hydrazine in electric discharge decomposition of ammonia. Journal of the American Chemical Society, 1954, 76(10): 2618–2626
2. Henis J M. Nitrogen oxide decomposition process. US Patent

3983021, 1976

3. Neyts E C, Ostrikov K, Sunkara M K, Bogaerts A. Plasma catalysis: Synergistic effects at the nanoscale. Chemical Reviews, 2015, 115 (24): 13408–13446

4. Russ H, Neiger M, Lang J E. Simulation of micro discharges for the optimization of energy requirements for removal of NO_x from exhaust gases. IEEE Transactions on Plasma Science, 1999, 27(1): 38–39

5. Chang J S, Kostov K G, Urashima K, Yamamoto T, Okayasu Y, Kato T, Iwaizumi T, Yoshimura K. Removal of NF_3 from semiconductor-process flue gases by tandem packed-bed plasma and adsorbent hybrid systems. IEEE Transactions on Industry Applications, 2002, 36(5): 1251–1259

6. Whitehead J C. Plasma-catalysis the known knowns, the known unknowns and the unknown unknowns. Journal of Physics. D, Applied Physics, 2016, 49(24): 243001

7. Neyts E C, Bogaerts A. Understanding plasma catalysis through modelling and simulation—a review. Journal of Physics. D, Applied Physics, 2014, 47(22): 224010

8. Voter A F. Parallel replica method for dynamics of infrequent events. Physical Review B: Condensed Matter and Materials Physics, 1998, 57(22): R13985–R13988

9. Perez D, Uberuaga B P, Voter A F. The parallel replica dynamics method—coming of age. Computational Material Science, 2015, 100, part B, 90–103

10. Voter A F. A method for accelerating the molecular dynamics simulation of infrequent events. Journal of Chemical Physics, 1997, 106(11): 4665–4677

11. Voter A F. Hyperdynamics: Accelerated molecular dynamics of infrequent events. Physical Review Letters, 1997, 78(20): 3908–3911

12. Sörensen M R, Voter A F. Temperature-accelerated dynamics simulation of infrequent events. Journal of Chemical Physics, 2000, 112: 9599

13. Montalenti F, Voter A F. Exploiting past visits or minimum barrier knowledge to gain further boost in the temperature-accelerated dynamics method. Journal of Chemical Physics, 2002, 116(12): 4819

14. Bal K M, Neyts E C. Merging metadynamics into hyperdynamics: Accelerated molecular simulations reaching time scales from microseconds to seconds. Journal of Chemical Theory and Computation, 2015, 11(10): 4545–4554

15. Bal K M, Neyts E C. Direct observation of realistic-temperature fuel combustion mechanisms in atomistic simulations. Chemical Science (Cambridge), 2016, 7(8): 5280–5286

16. Fu C D, Oliveira L F L, Pfaendtner J. Assessing generic collective variables for determining reaction rates in metadynamics simulations. Journal of Chemical Theory and Computation, 2017, 13(3): 968–973

17. Neyts E C, Brault P. Molecular dynamics simulations for plasma-surface interactions. Plasma Processes and Polymers, 2016, 14(1-2): 1600145

18. Shibuta Y, Maruyama S. Molecular dynamics simulation of formation process of single-walled carbon nanotubes by CCVD method. Chemical Physics Letters, 2003, 382(3-4): 381–386

19. Ding F, Bolton K, Rosén A. Nucleation and growth of single-walled

20. Neyts E C, Shibuta Y, van Duin A C T, Bogaerts A. Catalyzed growth of carbon nanotube with definable chirality by hybrid molecular dynamics—force biased Monte Carlo simulations. ACS Nano, 2010, 4(11): 6665–6672

21. Page A J, Yamane H, Ohta Y, Irle S, Morokuma K. QM/MD simulation of SWNT nucleation on transition-metal carbide nanoparticles. Journal of the American Chemical Society, 2010, 132(44): 15699–15707

22. Amara H, Bichara C, Ducastelle F. Understanding the nucleation mechanisms of carbon nanotubes in catalytic chemical vapor deposition. Physical Review Letters, 2008, 100(5): 056105

23. Zhao J, Martinez-Limia A, Balbuena P B. Understanding catalysed growth of single-wall carbon nanotubes. Nanotechnology, 2005, 16 (7): S575–S581

24. Khalilov U, Bogaerts A, Neyts E C. Atomic scale simulation of carbon nanotube nucleation from hydrocarbon precursors. Nature Communications, 2015, 6: 10306

25. Elliott J A, Shibuta Y, Amara H, Bichara C, Neyts E C. Atomistic modelling of CVD synthesis of carbon nanotubes and graphene. Nanoscale, 2013, 5(15): 6662–6676

26. Page A J, Ding F, Irle S, Morokuma K. Insights into carbon nanotube and graphene formation mechanisms from molecular simulations: A review. Reports on Progress in Physics, 2015, 78(3): 036501

27. Neyts E C. PECVD growth of carbon nanotubes: From experiment to simulation. Journal of Vacuum Science & Technology B Microelectronics and Nanometer Structures, 2012, 30: 030803

28. Meyyappan M. A review of plasma enhanced chemical vapour deposition of carbon nanotubes. Journal of Physics. D, Applied Physics, 2009, 42(21): 213001

29. Diega G G, Gilbert D M, Javier A, Perla B B. Dynamic evolution of supported metal nanocatalyst/carbon structure during single-walled carbon nanotube growth. ACS Nano, 2012, 6(1): 720–735

30. Diarra M, Zappelli A, Amara H, Ducastelle F, Bichara C. Importance of carbon solubility and wetting properties of nickel nanoparticles for single wall nanotube growth. Physical Review Letters, 2012, 109(18): 185501

31. Neyts E C, van Duin A C T, Bogaerts A. Insights in the plasma assisted growth of carbon nanotubes through atomic scale simulations: Effect of electric field. Journal of the American Chemical Society, 2012, 134(2): 1256–1260

32. Mees M J, Pourtois G, Neyts E C, Thijsse B J, Stesmans A. Uniform-acceptance force-bias Monte Carlo method with time scale to study solid-state diffusion. Physical Review B: Condensed Matter and Materials Physics, 2012, 85(13): 134301

33. Bal K M, Neyts E C. On the time scale associated with Monte Carlo simulations. Journal of Chemical Physics, 2014, 141(20): 204104

34. Timonova M, Groenewegen J, Thijsse B J. Modeling diffusion and phase transitions by a uniform-acceptance force-bias Monte Carlo method. Physical Review B: Condensed Matter and Materials Physics, 2010, 81(14): 144107

35. Neyts E C, Bogaerts A. Combining molecular dynamics with Monte Carlo simulations: Implementations and applications. Theoretical

Chemistry Accounts, 2013, 132(2): 1320

36. Neyts E C, Thijsse B J, Mees M J, Bal K M, Pourtois G. Establishing uniform acceptance in force biased Monte Carlo simulations. Journal of Chemical Theory and Computation, 2012, 8(6): 1865–1869

37. Neyts E C, van Duin A C T, Bogaerts A. Changing chirality during single-walled carbon nanotube growth: A reactive molecular dynamics/Monte Carlo study. Journal of the American Chemical Society, 2011, 133(43): 17225–17231

38. Kato T, Hatakeyama R. Formation of freestanding single-walled carbon nanotubes by plasma-enhanced CVD. Chemical Vapor Deposition, 2006, 12(6): 345–352

39. Nozaki T, Karatsu T, Ohnishi K, Okazaki K. A pressure-dependent selective growth of single-walled and multi-walled carbon nanotubes using plasma enhanced chemical vapor deposition. Carbon, 2010, 48(1): 232–238

40. Neyts E C. On the role of ions in plasma catalytic carbon nanotube growth: A review. Frontiers of Chemical Science and Engineering, 2015, 9(2): 154–162

41. Neyts E C, Ostrikov K, Han Z J, Kumar S, van Duin A C T, Bogaerts A. Defect healing and enhanced nucleation of carbon nanotubes by low-energy ion bombardment. Physical Review Letters, 2013, 110(6): 065501

42. Neyts E C, Bogaerts A. Ion irradiation for improved graphene network formation in carbon nanotube growth. Carbon, 2014, 77: 790–795

43. Shariat M, Hosseini S I, Shokri B, Neyts E C. Plasma enhanced growth of single walled carbon nanotubes at low temperature: A reactive molecular dynamics simulation. Carbon, 2013, 65: 269–276

44. Shariat M, Shokri B, Neyts E C. On the low-temperature growth mechanism of single walled carbon nanotubes in plasma enhanced chemical vapor deposition. Chemical Physics Letters, 2013, 590: 131–135

45. Chen H L, Lee H M, Chen S H, Chao Y, Chang M B. Review of plasma catalysis on hydrocarbon reforming for hydrogen production—interaction, integration and prospects. Applied Catalysis B: Environmental, 2008, 85(1-2): 1–9

46. Van Durme J, Dewulf J, Leys C, Van Langenhove H. Combining non-thermal plasma with heterogeneous catalysis in waste gas treatment: A review. Applied Catalysis B: Environmental, 2008, 78 (3-4): 324–333

47. Kim H H, Ogata A. Nonthermal plasma activates catalyst: From current understanding and future prospects. European Physical Journal Applied Physics, 2001, 55(1): 13806

48. Zhang Y R, Van Laer K, Neyts E C, Bogaerts A. Can plasma be formed in catalyst pores? A modeling investigation. Applied Catalysis B: Environmental, 2016, 185: 56–67

49. Zhang Y R, Neyts E C, Bogaerts A. Influence of the material dielectric constant on plasma generation inside catalyst pores. Journal of Physical Chemistry C, 2016, 120(45): 25923–25934

50. Van Laer K, Bogaerts A. Fluid modelling of a packed bed dielectric barrier discharge plasma reactor. Plasma Sources Science & Technology, 2016, 25(1): 015002

51. Van Laer K, Bogaerts A. Improving the conversion and energy efficiency of carbon dioxide splitting in a zirconia-packed dielectric barrier discharge reactor. Energy Technology (Weinheim), 2015, 3 (10): 1038–1044

52. Zhang Y, Wang H Y, Jiang W, Bogaerts A. Two-dimensional particle-in-cell/Monte Carlo simulations of a packed-bed dielectric barrier discharge in air at atmospheric pressure. New Journal of Physics, 2015, 17(8): 083056

53. Neyts E C, Bal K M. Effect of electric fields on plasma catalytic hydrocarbon oxidation from atomistic simulations. Plasma Processes and Polymers, 2017, 14(6): e1600158

54. Somers W, Bogaerts A, van Duin A C T, Neyts E C. Plasma species interacting with nickel surfaces: Towards an atomic scale understanding of plasma-catalysis. Journal of Physical Chemistry C, 2012, 116(39): 20958–20965

55. Somers W, Bogaerts A, van Duin A C T, Huygh S, Bal K M, Neyts E C. Temperature influence on the reactivity of plasma species on a nickel catalyst surface: An atomic scale study. Catalysis Today, 2014, 211: 131–136

56. Somers W, Bogaerts A, van Duin A C T, Neyts E C. Interactions of plasma species on nickel catalysts: A reactive molecular dynamics study on the influence of temperature and surface structure. Applied Catalysis B: Environmental, 2014, 154-155: 1–8

57. Neyts E C. Plasma-surface interactions in plasma catalysis. Plasma Chemistry and Plasma Processing, 2016, 36(1): 185–212

58. Halonen L, Bernasek S L, Nesbitt D J. Reactivity of vibrationally excited methane on nickel surfaces. Journal of Chemical Physics, 2001, 115(12): 5611–5619

59. Jackson B, Nave S. The dissociative chemisorption of methane on Ni(111): The effects of molecular vibration and lattice motion. Journal of Chemical Physics, 2013, 138(17): 174705

60. Shirazi M, Neyts E C, Bogaerts A. DFT study of Ni-catalyzed plasma dry reforming of methane. Applied Catalysis B: Environmental, 2017, 205: 605–614

61. Huygh S, Neyts E C. Adsorption of C and CH_x radicals on anatase (001) and the influence of oxygen vacancies. Journal of Physical Chemistry C, 2015, 119(9): 4908–4921

62. Huygh S, Bogaerts A, Neyts E C. How oxygen vacancies activate CO_2 dissociation on TiO_2 anatase (001). Journal of Physical Chemistry C, 2016, 120(38): 21659–21669